

## Research article

# Pyrolytic evaluation of essential oil industry waste: Effect of pyrolysis temperature on bio-oil composition

Sourodipto Modak <sup>a</sup> , Priyanka Katiyar <sup>a,\*</sup> , Dhrubajyoti Talukdar <sup>b</sup>, Bappaditya Gole <sup>b</sup>

<sup>a</sup> Department of Chemical Engineering, Shiv Nadar Institution of Eminence, Delhi, NCR, India

<sup>b</sup> Department of Chemistry, Shiv Nadar Institution of Eminence, Delhi, NCR, India

## ARTICLE INFO

### Keywords:

Bio-oil  
Essential oil industry waste  
Slow-pyrolysis  
GC-MS analysis  
NMR characterization

## ABSTRACT

The essential oil industry, a rapidly growing sector driven by its value-added applications, generates substantial amount of waste that contribute to land pollution and open dumping, highlighting the urgent need for effective waste management strategies. In this study, spent carrot seed waste (SCSW), a common byproduct of the essential oil industry, was pyrolytically evaluated at various temperatures (300–500 °C) to produce bio-oil. The proximate analysis of SCSW showed high volatile matter 71 % along with high ash content 13 %. XRF analysis of SCSW revealed the presence of alkali, alkaline and transition metals, which can act as an inherent catalytic site for the breaking of larger bio-oil compounds. SCSW contains substantial amounts of cellulose (32 %), hemicellulose (28 %) and lignin (27 %) along with extractives (12 %). TGA and DTG analysis exhibited the active devolatilization zone between 250 and 500 °C with weight loss of 50 %. Upon subjecting SCSW to pyrolysis at various temperature, the maximum amount of bio-oil was obtained i.e., 16 wt% at 500 °C. The GC-MS analysis revealed that notable amounts of cyclic ketones (42–50 %) were present in the SCSW-bio-oils, formed under the influence of metallic sites in the SCSW. These cyclic ketones mainly 1,3-Cyclopentanedione, holds the potential to be used for drug development and chemical probes applications. Increase in pyrolysis temperatures showed significant reduction in hydroxy-ketones and furanics but in contrast, there is the significant increment in cyclic hydrocarbons and anhydrosugars in the bio-oil. NMR analysis revealed highest aliphatic, aromatic and carbohydrate nature at 500 °C.

## 1. Introduction

Fossil fuels, particularly crude oil, natural gas, and coal have played a significant role in shaping modern civilization and driving remarkable progress in human society. However, the excessive use of these resources has led to their depletion, contributing to the ongoing energy crisis (Perera, 2018). In 2023, India imported petroleum crude oil and associated goods with a total value of approximately 16 trillion Indian Rupees (INR), which represents a significant financial burden ("India: petroleum products import value 2023 | Statista," n.d.). This highlights the urgent need for alternatives to replace fossil fuels. Lignocellulosic biomass or waste biomass has shown a potential as a replacement of fossil fuels and is currently considered a sustainable feedstock for biofuel production (Adewuyi, 2022; Preethi et al., 2021). Various type of waste biomass including the waste produced by municipalities (food waste) or industries (agro-industrial waste) can be repurposed to provide energy security as well as less carbon footprint (Yaashikaa et al., 2022).

One of the primary agro-industrial wastes generated these days are solid biowastes produced after extraction of essential oil such as fenugreek oil, clove oil, ginger oil etc. Due to a transition to a contemporary and healthy lifestyle, the demand for essential oils is increasing, leading to a rise in the amount of solid waste produced by the essential oil industry. According to the survey by Market Research Future, the essential oil market is expected to grow with a CAGR of 11.8 % from 2022 to 2027 with the fastest rate of growth expected in developing nations like India and China (Abu Bakar et al., 2020; "Essential Oils Market Key Drivers, Restraints and Winning Strategies | MarketsandMarkets™," n. d.). Given that the essential oil content in a solid matrix typically ranges from 5 to 20 %, approximately 80–95 % of the material remains as waste. This byproduct is commonly disposed of in landfills, leading to environmental concerns such as air and land pollution (Abu Bakar et al., 2020). As these wastes are natural products, they possess the characteristics of lignocellulosic biomass, along with various inorganic components, making them highly suitable for use as feedstock to produce biofuel and

\* Corresponding author.

E-mail address: [priyanka@snu.edu.in](mailto:priyanka@snu.edu.in) (P. Katiyar).

value-added chemicals via pyrolysis technique.

Few researchers have worked on the pyrolysis of various oil extraction residues generated from agro-industries. Abu Bakar et al. (2020) worked on the pyrolysis of defatted lemon myrtle at pyrolysis temperatures ranging from 350 to 550 °C to produce the superior quality bio-oil which contains the acids, phenolics, furans. In another work, industrial spent ginger waste was pyrolyzed via microwave pyrolysis within the temperature range 200–300 °C, which yielded the bio-oil having mainly furanic, aliphatic & aromatic substituents to be used as value added chemicals (Gao et al., 2021). Further, the bio-oil obtained from the pyrolysis of spent coffee residues showed the major presence of lipids and hydrocarbons with the maximum bio-oil yield of 61 % (Kelkar et al., 2015). Casoni et al. (2019) pyrolytically evaluated spent sunflower waste at 450 °C to produce bio-oil rich in furfural, acetic acid and levoglucosan. Li et al. (2021) carried out the pyrolysis of post extraction sesame residue at different pyrolysis temperatures ranging from 350 to 650 °C to produce the bio-oil containing majorly nitrogenated compounds, acids and phenols (Li et al., 2021). Researchers have explored the pyrolytic valorization of defatted edible seed wastes (such as mustard, soybean, groundnut, sunflower, and flaxseeds) as well as non-edible seed wastes (including castor, cotton, neem, karanja, and mahua) (Rajpoot et al., 2022). However, there are limited studies on the valorization of waste from the essential oil industry, with notable examples being the pyrolytic valorization of spent lemon myrtle and spent citronella waste (Abu Bakar et al., 2020; Kaur et al., 2022). Additionally, no study has addressed the use of spent carrot seed waste (SCSW), generated after the extraction of oil, for bio-oil production through pyrolysis at various temperatures. Owing to value-added properties of carrot seed oil (antioxidant, antimicrobial, and antifungal effects) (Modak et al., 2023), the market for carrot seed oil is anticipated to grow significantly by 2029 particularly in America, Europe, East Asia, South Asia, Middle East, and Africa (Sieniawska et al., 2016). This growing demand for carrot seed oil will result in the bulk production of spent carrot seed waste, which could serve as a potential feedstock for bio-oil production.

The present study examines the characteristics of spent carrot seed waste (SCSW) for its potential use as feedstock in the pyrolysis process, employing proximate, ultimate, lignocellulosic, TGA, and XRF analyses. Further, the pyrolytic evaluation of SCSW is carried out at various pyrolysis temperatures (300, 400 & 500 °C) to produce bio-oil. This study majorly focuses on effect of pyrolysis temperatures on bio-oil quantity and composition including mechanistic understanding using GC-MS and NMR techniques.

## 2. Material and methods

### 2.1. Procurement of SCSW

The SCSW was procured from Rajeshwari essential oil industry, India. The samples were subjected to oven-dry for 12 h to remove the unbound moisture from the samples. After the oven dry, the dried samples were packed and kept for characterization and pyrolysis evaluation.

### 2.2. Physico-chemical characterization of SCSW

For identification of physico-chemical properties of SCSW prior to the pyrolytic evaluation, the samples were subjected to proximate, ultimate, and TG analysis (Modak et al., 2023). In the proximate analysis, the % moisture, ash and volatile content was evaluated according to ASTM D-3137, ASTM D-3174-11 and ASTM D3175-20 respectively. The ultimate analysis was carried out in Thermo Finnigan Flash 1112 Series Elemental analyser. The Thermogravimetric (TG) analysis of the SCSW sample was performed using a TGA/DTG analyzer (TA Instruments, USA) over a temperature range of 25–800 °C. The analysis was conducted at a heating rate of 10 °C/min under a constant nitrogen flow of

100 mL/min. The ash composition in the SCSW was evaluated using XRF analysis (Modak et al., 2023) using WD-XRF (AxiosMax-Pananlytical). Before analysis, the SCSW sample was oven-dried at 105 °C for 12 h to eliminate residual moisture, then ground to achieve a particle size below 75 µm. The resulting powder was mixed with boric acid as a binding agent and compressed into pellets under 30 tons of pressure for 1 min. The prepared pellet was then placed in a sample holder and loaded into the XRF analyzer for further analysis. The lignocellulosic analysis was carried out in accordance to the method proposed by Tappi T222 om-02 (Li et al., 2004; Varma and Mondal, 2016). Extractives were isolated from the SCSW sample using the Soxhlet extraction method. For this, 1 g of SCSW (initial mass: M<sub>0</sub>) was placed in a cellulose thimble, and a solvent mixture of benzene and ethanol in a 2:1 (v/v) ratio was added to a round-bottom flask. The extraction was carried out at 60 °C for 4 h. Further, the sample was dried, cooled, and weighed (mass: M<sub>1</sub>) and the percentage of extractives was calculated using equation (1).

$$\% \text{ Extractives} = \frac{M_0 - M_1}{M_0} \times 100 \quad (1)$$

To determine the hemicellulose content, an alkali treatment method was employed by treating 1 g of the extractive-free SCSW (M<sub>1</sub>) with 150 mL of 0.5 M NaOH in a reflux system heated at 110 °C for 4 h. After the reaction, the mixture was filtered and washed repeatedly with deionized water until neutral. The resulting filter cake was dried in a hot air oven at 100 °C for 10 h, cooled, and weighed to obtain M<sub>2</sub>. The hemicellulose content was calculated using equation (2).

$$\% \text{ Hemicellulose} = \frac{M_1 - M_2}{M_0} \times 100 \quad (2)$$

Lignin content of SCSW was determined via acid hydrolysis to isolate the acid-insoluble lignin fraction and hydrolyze the carbohydrate components. In this step, 1 g of the extractive-free SCSW sample was treated with 15 mL of 72 % sulfuric acid and left to hydrolyze for 2 h. The mixture was then diluted with deionized water to reduce the acid concentration to 3 %, followed by boiling for 3.5 h. Afterward, the acid-insoluble lignin was allowed to settle, filtered through a Gooch crucible, and thoroughly washed with hot water until the pH was neutral. The lignin residue was oven-dried at 106 °C for 14 h, then transferred to a silica crucible to perform ash correction in accordance with ASTM D3174-11. The lignin content was calculated using equation 3

$$\% \text{ Lignin} = \frac{\text{Weight of acid insoluble lignin(g)}}{\text{Initial weight of SCSW (g)}} \times 100 \quad (3)$$

### 2.3. Pyrolysis setup

To carry out pyrolysis of SCSW, semi-continuous fixed bed batch reactor was used as shown in Fig. 1. The tubular semi-continuous reactor, made of Inconel 665 alloy, was equipped with a feed hopper positioned at the top (3). Additionally, the reactor has a stainless steel (SS) socket (7), housed with a removable cylindrical steel tube (6) at the top. This removable SS socket was provided to hold the biomass and to remove biochar from the reactor. The SS socket was encased with a threaded SS socket (8) to provide support and a connection between the condenser (10) and reactor. The reactor was surrounded with 3 nichrome heaters (9), connected to PID controller. There were 2 K-type thermo-couples installed in the reactor system: (i) inside the reactor, and (ii) at vicinity of the heater.

Once the SCSW (70 g) was fed to the reactor through the hopper, the heaters were turned on along with N<sub>2</sub> gas (200 ml/min) fed from the top to maintain the inert environment. The heaters were gradually heated from room temperature to 80 °C and maintained for 10 min to stabilize the heating coils and mitigate thermal lag within the heaters. Subsequently, the temperature was increased to desired temperature from 80 °C at a fixed heating rate of 10 °C/min and held steady till process was complete. The bio-oil was collected at the bottom in the 2-neck flask

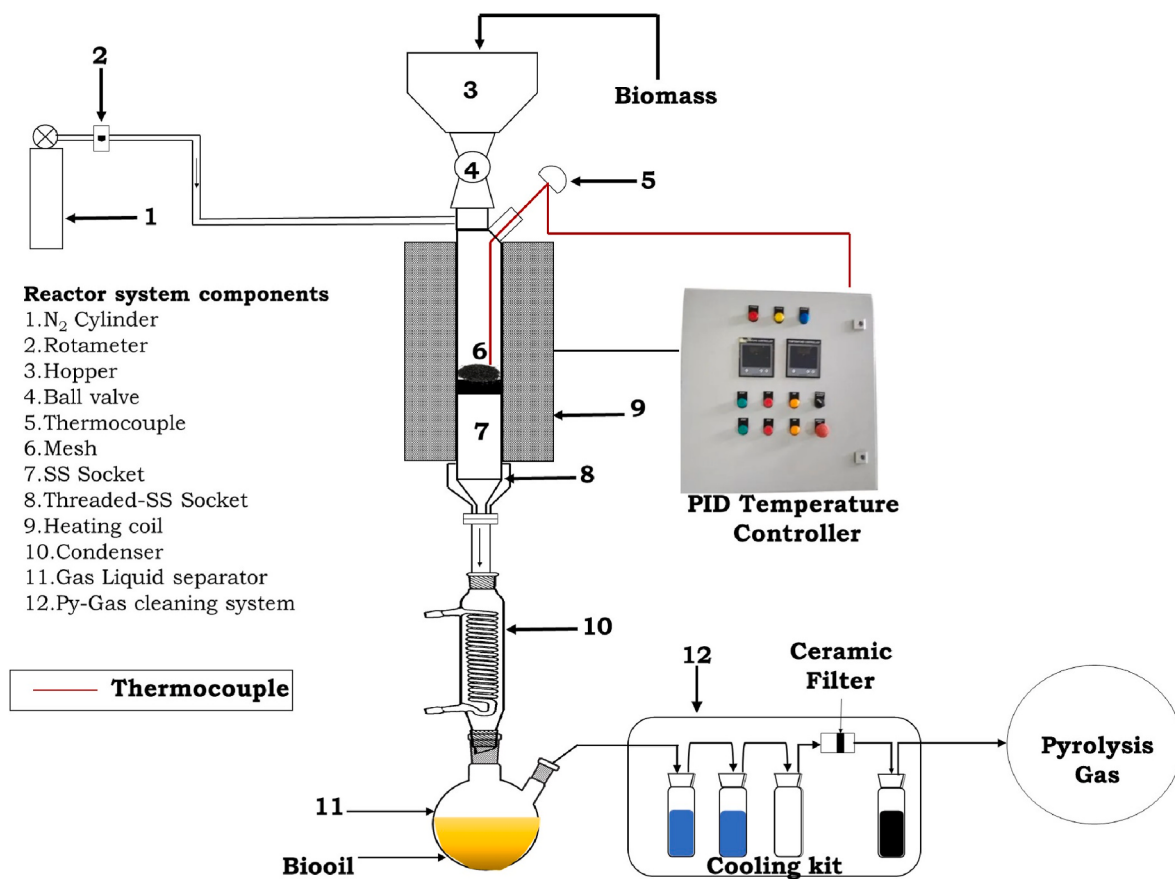


Fig. 1. Schematic diagram of pyrolysis reactor.

(11) after the cooling of condensable gases in condenser. The % yield of bio-oil is calculated according to equation (4).

$$\text{Bio-oil (wt\%)} = \frac{\text{Weight of bio-oil obtained (g)}}{\text{Initial weight of SCSW (g)}} \times 100 \quad (4)$$

#### 2.4. Water content analysis, purification and characterization of SCSW bio-oil

The water content in the SCSW bio-oil was evaluated using Karl Fisher Titrator (Spectralab MA-101C). The bio-oil samples were initially dissolved in Acetone (HPLC grade, Qualigens) in a ratio of 1: 10 (Bio-oil: Acetone). Further, 1 g of Na<sub>2</sub>SO<sub>4</sub> (Qualigens) was added in the mixture to adsorb the free water content in the bio-oil and stirred vigorously. The finally purified bio-oil samples were sealed for GC-MS and NMR analysis. GC-MS analysis of SCSW bio-oil samples was carried out in Agilent 5977B GC/MSD where HP-5MS capillary column (30m × 0.25 mm, 0.25 µm) was used. The purified bio-oils were dissolved in Acetone (HPLC grade) and injected at a split ratio of 1:20 and ramping rate at 2 °C/min. The initial and final temperatures were maintained at 60 and 300 °C, respectively and helium was used as a carrier gas at a flow rate of 3 ml/min. After the peaks were obtained, organic compounds matching with respectable peaks were identified using NIST-MS search software.

To analyse the overall molecularity of the bio-oil, NMR analysis was conducted. The 400 MHz Bruker NMR instrument was used for <sup>1</sup>H and <sup>13</sup>C-NMR spectroscopy. The purified bio-oil sample of around 200 µl was dissolved in DMSO-d<sub>6</sub> (Eurisotop). The <sup>13</sup>C-NMR spectroscopy was conducted with a scanning range of 0–225 ppm at 100 MHz and a temperature of 23 °C. For the <sup>1</sup>H-NMR spectroscopy, a scanning range of 1–10 ppm was utilized at 400 MHz. Subsequently, the peaks were examined using the area integration approach in Topspin software (Bruker, Germany) to identify distinct hydrogen and carbon

environments across various molecules in the bio-oil.

### 3. Results and discussions

#### 3.1. Physicochemical characterization of SCSW

Table 1 shows the proximate, ultimate and lignocellulosic analysis of SCSW, where proximate analysis showed higher volatile content (71.3 %), comparable with the volatile content of rice straw and bamboo leaves i.e., 73 % and 70 % (Biswas et al., 2017; Huang et al., 2011). The proximate analysis also revealed that SCSW possesses a substantial ash content of approximately 13 %, comparable to the 12.6 % ash percentage of sugarcane peel (Huang et al., 2011). Higher volatile matter in the biomass favours the formation of volatile vapors, resulting in enhanced bio-oil production, whereas presence of significant ash facilitates the cracking reactions of larger molecules during the bio-oil formation (Cai et al., 2017). The inorganic constituents of SCSW ash, shown in Table 1, revealed mostly alkali, alkaline and transition metals such as Na, Mg, Si, Fe, K and Ca. These metallic constituents may be responsible for catalytic characteristics during the pyrolysis of SCSW (Wang et al., 2022).

The fixed carbon content in SCSW is comparatively lesser than that of conventional lignocellulosic biomass including coffee husk (22 %), *Eucalyptus urophylla* (16 %) (Veiga et al., 2017), but comparable with the sugarcane bagasse (5 %) and corn cob (7 %) (Biswas et al., 2017; Huang et al., 2011). Less fixed carbon content leads to the lesser formation of char during pyrolysis process (Basu, 2018). Ultimate analysis as given in Table 1, exhibited notable amount of carbon and oxygen i.e., 39 % and 39 % respectively due to presence of biopolymers such as cellulose, hemicellulose and lignin in SCSW. In contrast, hydrogen and nitrogen content are low i.e. 5.82 %, 3.69 % whereas sulphur is present in

**Table 1**

Proximate, ultimate and lignocellulosic analysis of SCSW.

Proximate Analysis		Ultimate analysis			Lignocellulosic analysis					
Moisture ( $\pm 3\%$ )	6.9	C (%)	39.2	Extractives ( $\pm 2.5\%$ )	12					
Ash ( $\pm 3\%$ )	13.3	H (%)	5.87	Cellulose ( $\pm 2.5\%$ )	32					
Volatile Matter ( $\pm 3\%$ )	71.3	O (%)	39.02	Hemicellulose ( $\pm 2.5\%$ )	28					
Fixed Carbon ( $\pm 3\%$ )	8.2	N (%)	3.69	Lignin ( $\pm 2.5\%$ )	27					
HHV (MJ/kg)	14.02	S (%)	0.48							
XRF analysis of SCSW ash										
Oxides	Na <sub>2</sub> O	MgO	Fe <sub>2</sub> O <sub>3</sub>	SiO <sub>2</sub>	P <sub>2</sub> O <sub>5</sub>	SO <sub>3</sub>	K <sub>2</sub> O	CaO	Al <sub>2</sub> O <sub>3</sub>	TiO <sub>2</sub>
Weight%	12.1	4.2	5.3	14.6	7.1	7.3	7.9	29.0	3.5	0.28
										MnO
										0.28

negligible amount i.e. 0.48 %. The lower levels of sulphur in the biomass reduces corrosion and increases the shelf life of the pyrolysis reactor (Mishra and Mohanty, 2018). The lignocellulosic analysis of SCSW shows 32 % of cellulose, 28 % of hemi-cellulose, 27 % of lignin and 12 % of extractives, comparable with the typical biomasses such as cotton stalk and Moringa pod (Fadeyi and Akiode, 2023; Saravanan et al., 2023). The extractives in essential oil industry waste are the residual oil species in the biomass, left after the extraction. These compounds are mainly polar and nonpolar fatty compounds and terpenoids.

TG and DTG analysis of SCSW, given in Fig. 2 and Table 2, exhibit 3 zones of mass loss; 1st zone ranges from 50 to 200 °C and accounts for 4 % of weight loss. 2nd and 3rd zone are observed from 200 to 450 °C and 450–800 °C respectively, displaying 50 % and 16 % of weight loss. 1st zone represents the dehydration of trapped moisture, evaporation of water-soluble lighter volatiles or hydrocarbons along with start of lignin degradation (Roostazadeh et al., 2022) whereas 2nd zone corresponds to active devolatilization stage or active pyrolysis zone where major decomposition of hemicellulose, cellulose and lignin take place (Priyanka et al., 2014; Saikia and Bardalai, 2018). Hemicellulose degradation takes place between 200 and 280 °C while cellulose gets decomposed in 280–360 °C range and the % mass loss of lignin becomes evident near 425 °C. The 3rd zone corresponds to the remaining lignin decomposition and char formation.

The DTG analysis shows peaks of biopolymer degradation such as hemicellulose at 260 °C (mild distinct), cellulose at 325 °C (sharp and distinct) and a tiny submerged peak at 425 °C corresponding to lignin decomposition and initiation of char combustion (Yi et al., 2013). The hemicellulose exhibits branched structure composed of polysaccharides, generally shows mild distinct degradation peak between 250 and 300 °C, whereas cellulose exhibits linear polymeric structure of glucose, which is highly ordered and exhibits distinct thermal degradation between 300 and 400 °C (Varol and Mutlu, 2023). Unlike cellulose and hemicellulose, lignin displays a broad degradation range from 200 to

**Table 2**

Weight loss (%) in nth thermal zone.

Thermal Zone	T <sub>i</sub> (°C)	T <sub>f</sub> (°C)	Weight loss (%)
1st Zone	50	200	4
2nd Zone	200	450	50
3rd Zone	450	800	16

T<sub>i</sub> – Initial Temperature of respective nth zone, T<sub>f</sub> – Final temperature of nth zone.

500 °C due to its complex molecular structure composed of aromatic units such as p-hydroxyphenyl, guaiacyl, and syringyl (Collard and Blin, 2014; Roostazadeh et al., 2022). In the third stage, continuous thermal degradation of residual lignin biopolymer or high molecular weight components could be seen at a much lower rate (no distinct degradation) due to degradation of heavier volatiles, cracking of C–C bonds and char formation (Modak et al., 2023). From TG and DTG analysis, it is evident that maximum yield of bio-oils will be produced due to devolatilization within the temperature range from 300 to 500 °C.

### 3.2. Effect of pyrolysis temperatures on bio-oil yield

Fig. 3 presents the effect of pyrolysis temperature on the bio-oil yield of SCSW. It can be noticed that increase in pyrolysis temperatures from 300 to 500 °C increased the bio-oil yield from 13 to 16.4 wt%.

The rise in temperature facilitates the enhanced thermal breakdown of indigenous compounds found in biomass, including cellulose, hemicellulose, and lignin. This phenomenon has resulted in an upsurge in the production of liquid product of bio-oil i.e. bio-oil. (Maulinda et al., 2023). However, the yield of bio-oil from SCSW pyrolysis is comparatively lower than that of other agro-industrial waste i.e. 27 % bio-oil yield for *Lemon Myrtle* waste @ 500 °C (Abu Bakar et al., 2020) and 30 % bio-oil yield for spent *Cymbopogon flexuosus* @ 450 °C (Deshmukh

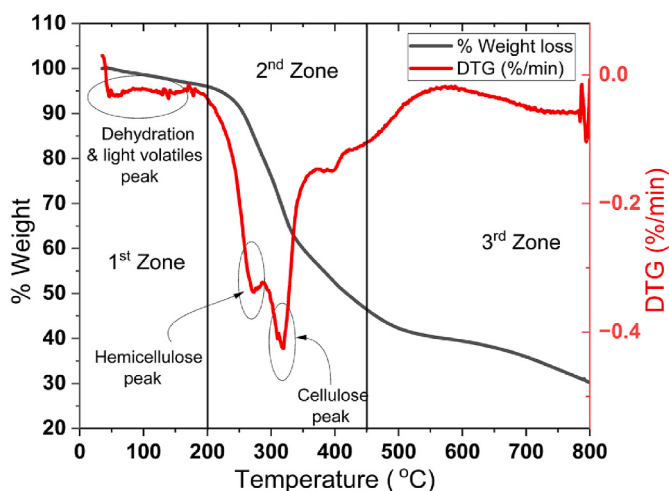


Fig. 2. TGA/DTG analysis of SCSW.

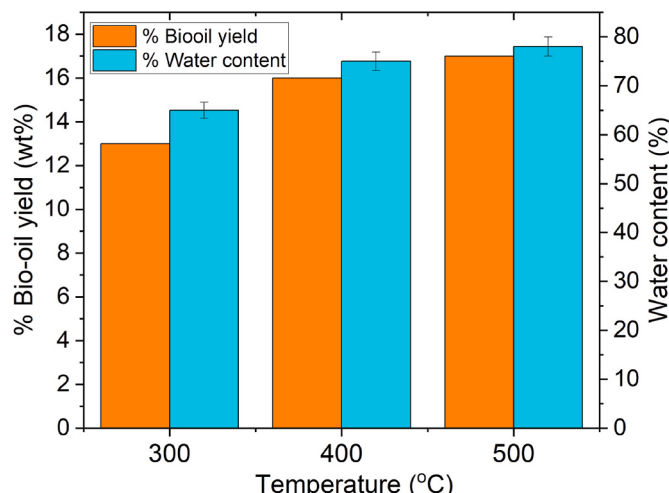


Fig. 3. SCSW bio-oil yield and % water content at various pyrolysis temperature.

**et al., 2015**). This is majorly due to presence of metallic species in the SCSW which promoted the secondary reactions (**Vasu et al., 2020a**). Likewise, it is noticed that the water content also increased with increase in pyrolysis temperature, mainly due to the enhanced dehydration reactions at higher temperature those release water as byproduct (500 °C) (**Kakku et al., 2023; Silva et al., 2016**).

### 3.3. GC-MS analysis of SCSW bio-oils

The effect of temperature (300, 400, 500 °C) on the composition of SCSW bio-oil was carried out by analyzing bio-oils using GCMS and compounds identified are tabulated in **Table 3**. The SCSW bio-oils contain wide varieties of compounds including hydroxy ketones, nitrogenated compounds, oxygen containing cyclic aliphatics, ketones (cyclic and aliphatic), furanics, phenolics, aromatics, aliphatic, cyclic hydrocarbons, anhydrosugars, esters and fatty acids. The hydroxy ketones which include 2-Propanone,1-hydroxy- majorly were reduced significantly from 15.21 to 4.70 % with rise in temperature from 300 to 500 °C. A considerable amount of N-containing compounds were produced due to presence of %N in SCSW (3.7 %) as shown in **Table 1**. The content of N-containing compounds increased notably from 6.6 to 13.28 % with an increase in temperature from 300 to 400 °C, however no significant variation was observed with further increase in temperature 500 °C.

The oxygen containing cyclic compounds such as carotol and daucol varied mildly between 6.13 and 5.4 % in the SCSW-bio-oils with variation in temperature. Cyclic ketones containing 1,3-Cyclopentanedione majorly showed maximum presence in the SCSW-bio-oils ranging from 40 to 49 %. The aliphatic ketonic compounds or linear ketones such as 2-Butanone, 3-methyl- and 1-Propanone, 1-cyclopropyl- were only present in SCSW bio-oil obtained from the 300 °C. The linear alcohols such as 1-Butanol and 1,2,6-Hexanetriol showed the presence of <1 % in the bio-oils obtained at 300 and 400 °C but further increase in temperature from 400 to 500 °C increased its content from 0.5 to 2.24 %. Furanic compounds (2-Furanmethanol) were reduced from 9 to 5.57 % with increase in temperature from 300 to 400 °C however showed the variation of 1 % with further increase in temperature to 500 °C i.e., 6.47 %. Similarly, phenolic compounds (phenol and phenol.2-methoxy) were reduced from 11.3 to 7.7 % with increase in temperature from 300 to 400 °C but further increase in temperature to 500 °C increased the phenolic content to 11.3 %. Aromatic hydrocarbons (Toluene) showed a milder but constant presence in SCSW bio-oils i.e. 2 %.

The aliphatic hydrocarbons (butane and pentane derivative) showed the little traces (1 %) in the SCSW bio-oils. The cyclic hydrocarbons (cyclobutene) and anhydrosugars were increased continuously from 1.95 to 6.34 % and 0.92–3.26 % respectively with increase in temperature from 300 to 500 °C. It is noticeable that esters (1,2-Ethanediol, monoacetate and 2-Propanone, 1- (acetyloxy)) and fatty acids were absent at 300 °C, however present in noticeable amount at 400 and 500 °C.

### *3.4. Mechanistic analysis of variation in SCSW bio-oil composition*

This section presents the plausible mechanistic analysis of bio-oil compounds formation at different pyrolysis temperatures. Figs. 4 and 5 present the organic compounds distribution and plausible mechanism for the formation of compounds in SCSW bio-oils obtained at 300, 400 and 500 °C. It is seen that cyclic ketones cover the majority of the SCSW bio-oils obtained at different pyrolysis temperature ranging from 40 to 49 %. The typical cyclic ketones detected in the bio-oils including 1,3-Cyclopentanedione, 1,2,4-Cyclopentanetrione, Cyclohexanone, 4-ethyl and 1,2-Cyclopentanedione, 3-methyl were basically formed from cellulose and hemicellulose through multiple pathways as depicted in Fig. 5. At lower temperature (300 °C), the ring opening and cyclization of hemicellulose had led to the formation of cyclic ketones. Further increase in temperature to 400 °C activated the cellulose to undergo dehydration, decarboxylation, decarbonylation to form cyclic ketones

**Table 3**  
Consolidated GC-MS analysis of SCSW-bio-oils

Organic compound category	Compounds identified	% Area		
		BO-300	BO-400	BO-500
<b>Hydroxy ketones</b>	2-Propanone, 1-hydroxy-	14.01	6.05	4.18
	Acetoin	1.2	0.6	0
	2-Pentanone, 4-hydroxy-4-methyl-	0	0	0.52
	Total	15.21	6.65	4.7
<b>Nitrogen containing compound</b>	2-Butenal, dimethylhydrazone	0	4.28	4.13
	Propanenitrile, 3-	0	0	0.7
	Triethylenediamine	0	0	1.33
	N-Cyano-2-methylpyrrolidine	0	0	0.66
	N,N-Dimethylaminoethanol	2.14	2.05	1.44
	Nitro-tert-butyl-acetate	0.93	0.62	0
	Methanamine, N,N-dimethyl-, N-oxid	0	0	0
	2-Piperidinone, 1-methyl-	1.01	0	1.4
	3-Methyl-5-hydroxy-isoxazole -	0.67	0	0
	N,N-Dimethylaminoethanol	0	0	0
	Cyclohexanone, 2-(dimethylamino)	0	0.56	0
	2,5-Pyrrolidinedione, 1-methyl-	0	0.83	0
	Methanamine, N,N-dimethyl-, N-oxid	0	0	0
	Pyridine	0.88	1.32	1.31
	Pyrazine, methyl-	0.97	0	0.43
	1H-1,2,4-Triazole, 3-methyl-	0	0.69	0
	3-Aminopyridine	0	0.95	0
<b>Oxygen containing cyclic aliphatic compound</b>	Pyrazine, ethyl-	0	1.43	0
	1,3-Diazine	0	0	0.72
	9-Acridinamine	0	0.55	0
	Total	6.6	13.28	12.12
	6-Oxa-bicyclo[3.1.0]hexan-3-one	0	0.48	0
	Dianhydromannitol	2.97	2.28	0
	Isosorbide	0.99	0.49	0.87
	Carotol	0.76	0	3.02
	Daucol	0		0.73
	2-Ethyl-tetrahydropyran	1.41	0	0
<b>Ketones (Cyclic + aliphatic)</b>	2H-Pyran-2-one	0	0.58	0
	Oxirane, trimethyl	0	0.68	0.78
	Maltool	0	0	0
	Total	6.13	4.99	5.4
	Cyclopentanone	0	0	0.69
	1,3-Cyclopentanedione (Cyclic ketone)	32.84	45.34	39.79
	1,2,4-Cyclopentanetrione (Cyclic ketone)	3.7	2.12	0
	2-Cyclopenten-1-one, 2-methyl- (Cyclic ketone)	0.73	0	0
	3-Methylcyclopentane-1,2-dione (Cyclic ketone)	2.09	1.56	0
	2-Cyclopenten-1-one, 3-ethyl-2-hydroxy (Cyclic ketone)	1.03	0.86	0
<b>Linear alcohol</b>	1,2-Cyclopentanediene, 3-methyl- (Cyclic ketone)	0	0	1.57
	2-Butanone, 3-methyl- (Linear ketone)	1.05	0	0
	1-Propanone, 1-cyclopropyl- (Linear ketone)	3.16	0	0
	3-Penten-2-one, (Linear ketone)	0	0	0.77
	Total	44.6	49.88	42.82
	1-Butanol	0.85	0	0
	1,2,6-Hexanetriol	0	0.53	0
<b>Furanic compound</b>	1,2-Ethanediol	0	0	2.24
	Total	0.85	0.53	2.24
	2-Furanmethanol	6.39	4.73	4.39
	Ethanone, 1- (2-furanyl) -	0.98	0.84	0.7

*(continued on next page)*

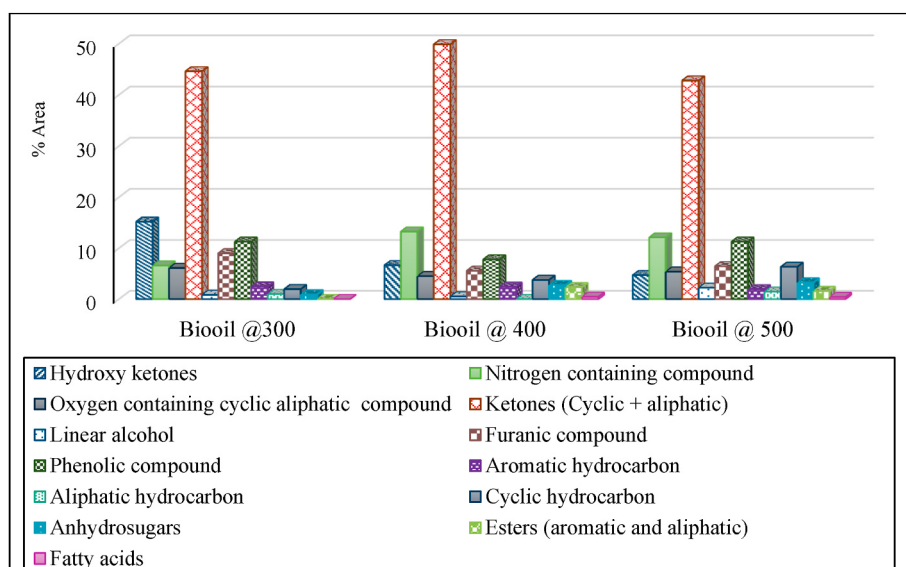
**Table 3 (continued)**

Organic compound category	Compounds identified	% Area		
		BO-300	BO-400	BO-500
Phenolic compound	Butyrolactone	1.65	0	1.38
	Total	9.02	5.57	6.47
	Phenol	6.56	4.48	5.27
	Phenol, 2-methoxy	2.49	2.05	2.78
	Phenol, 2,6-dimethoxy-	2.24	1.26	1.51
	p-Cresol	0	0	0.54
	Phenol, 4-ethyl-	0	0	0.49
Aromatic hydrocarbon	2-Methoxy-4-vinylphenol	0	0	0.69
	Total	11.29	7.79	11.28
	Toluene	2.46	2.42	1.93
	Total	2.46	2.42	1.93
	Aliphatic hydrocarbon			
	Butane, 2,3-dimethyl-	0.99	0	0
	1-Pentene, 2,3-dimethyl-	0	0	0.4
Cyclic hydrocarbon	2-Nonene, (E)	0	0	1.05
	Total	0.99	0	1.45
	Cyclobutene	0.81	1.79	1.39
	Bicyclo[2.1.0] pentane	0	0.88	1.38
	Cyclopropane, ethyl-	1.14	1.1	0.77
	Cyclobutane, methyl-	0	0	1.27
	Norbornadiene	0	0	0.66
Anhydrosugars	Cyclobutane 2-ethyl-1-methyl-3-propyl	0	0	0.88
	Total	1.95	3.77	6.35
	$\alpha$ -D-Mannopyranoside, methyl 3,6-anhydro-1,4:3,6-Dianhydroalpha-D glucopyranose -pyranose	0.92	0	0.61
	Total	0.92	2.77	3.26
	1,2-Ethanediol, monoacetate	0	0.47	0
	1,2-Ethanediol, diacetate	0	0.87	0
	Butanoic acid, 2-propenyl ester	0	0.47	0
Esters (Aromatic & aliphatic)	Benzoic acid, 4-ethoxy-, ethyl ester	0	0.53	0
	2-Propanone, 1-(acetoxy)	0	0	0.67
	2-Piperidincarboxylic acid, 1-acetyl-, ethyl ester	0	0	0.9
	Total	0	2.34	1.57
	Propanoic acid	0	0.47	0
	Acetic acid, (acetoxy)	0	0	0.41
	Total	0	0.47	0.41
Fatty acids				

(Li et al., 2022). Cellulose present in SCSW also produced anhydrosugars by the dehydration and these anhydrosugars had further undergone decarboxylation, decarbonylation due to presence of metallic constituents (Mg, Ca and Fe) in SCSW to form the light oxygenates such as cyclic ketones as illustrated in Fig. 5 (Hakeem et al., 2021; Hu and Gholizadeh, 2019). The content of hydroxy ketones was significantly decreased with an increase in temperature from 300 to 500 °C as shown in Fig. 4. The hydroxy ketones were formed by the ring opening and cracking rearrangement reaction of hemicellulose at 300 °C. Oxygen containing cyclic aliphatic compounds comprising of terpenoid and phenol derived compounds were also formed in SCSW bio-oils obtained at various pyrolysis temperatures. During pyrolysis, the bioactive compounds which were inherently present in the essential oil industry waste, got thermally activated to form carotol and daucol in the bio-oil. These bio-active compounds were not usually found in the pyrolysis bio-oil derived from conventional lignocellulosic biomass such as rice straw and woody biomass (Hsu et al., 2015) (Efika et al., 2018).

The furanic compounds decreased with an increase in temperature from 300 to 500 °C. At 300 °C, furanic compounds were formed by two ways (i) ring opening and cyclization of hemicellulose (ii) ring opening and cyclization of anhydrosugars as shown in Fig. 5 (Hu and Gholizadeh, 2019). These furanic compounds had further undergone dual reaction pathways, cracking and deoxygenation reaction to form aliphatic compounds (Rangel et al., 2023) and dehydration, rearrangement and oligomerization reaction to form phenolic compounds at higher pyrolysis temperatures (500 °C), resulting a decrease in their content (Hu et al., 2020). As noticed from Figs. 4 and 5, lignin had undergone thermal degradation and H-bond cleaving to form phenolic compounds under the catalytic influence of K at the 300 °C (Vasu et al., 2020b). Further these phenolic compounds exhibited deoxygenation reaction to form aromatic hydrocarbons due to metallic sites such as Fe, accounting 2 % in the SCSW bio-oils from 300 to 400 °C (Hu et al., 2021). At higher temperature (500 °C), the furanic compounds further undergo dehydration and rearrangement reaction to form phenolic compounds. The aliphatic hydrocarbons showed the presence of 1.5 % in the SCSW bio-oil obtained at 500 °C. The traces of these hydrocarbons are formed by the deoxygenation reaction of hydroxy ketone and furans under the influence of metallic traces and higher pyrolysis temperatures (Hu and Gholizadeh, 2019; Karnjanakom et al., 2020).

Increase in pyrolysis temperature from 300 to 500 °C showed an increment in the cyclic hydrocarbons due to cyclization of aliphatic hydrocarbon (Wan et al., 2022). The aromatic hydrocarbons such as

**Fig. 4.** Consolidated organic compounds in SCSW bio-oils at various temperatures.

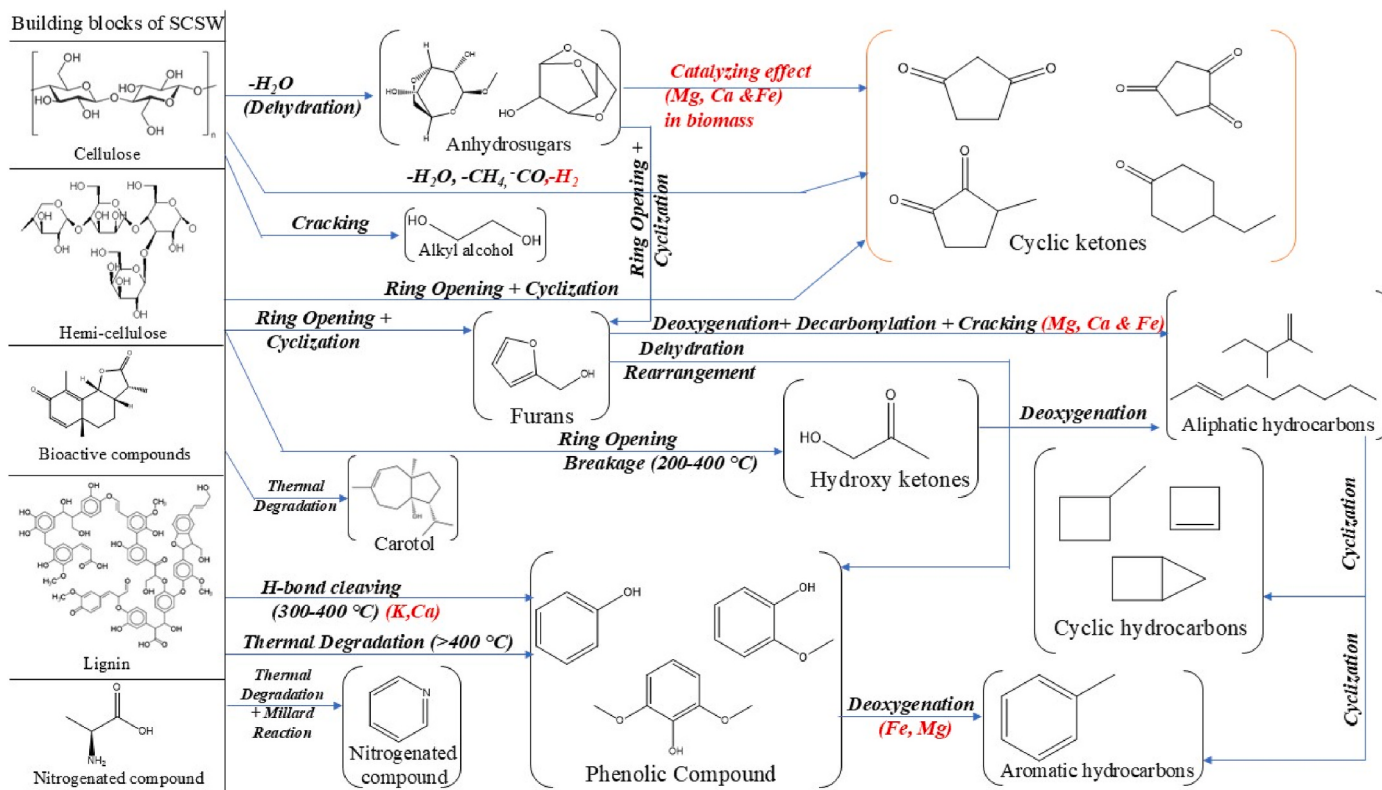


Fig. 5. Plausible mechanism for pyrolysis of SCSW at various pyrolysis.

toluene showed mild presence in the SCSW bio-oils ranging from 2.46 to 1.93 % due to cyclization of aliphatic hydrocarbons (Vuppala et al., 2023) and ash (Fe) assisted deoxygenation reaction of phenolic compounds (Zadeh et al., 2020). In SCSW bio-oils, there was the mild presence of linear alcohols as shown in Fig. 4, formed by the thermal degradation of cellulose present in SCSW (Wang et al., 2021) as shown in Fig. 5. Fig. 4 illustrates that SCSW-bio-oil contained a wide variety of nitrogenous ranging from 6.6 to 13.28 %. The inherent nitrogenated compounds found in the lignocellulosic biomass due to atmospheric deposition and agricultural fertilization had undergone thermal degradation or Maillard reactions to form these nitrogenated compounds in the SCSW bio-oil (Deshmukh et al., 2015; Gautam and Vinu, 2020).

Based on the above discussion, the optimum pyrolysis temperature of SCSW pyrolysis can be considered as 500 °C due to maximum bio-oil yield of 16.4 wt%. As far as the quality of the bio-oil at 500 °C is concerned, it has higher presence of ketones with increased amounts of cyclic hydrocarbons (6.35 %) and notable amounts of phenolic compounds (11.28 %). Later studies can be carried out at 500 °C by varying other pyrolysis parameters such as heating rates or influence of catalyst to further improve the quality of the SCSW bio-oil.

### 3.5. NMR analysis of SCSW bio-oils

Bio-oil is a mixture of variety of organic species, which is shown by GC-MS analysis. In-depth analysis and characterization of bio-oil is carried out using NMR spectroscopic methods which includes <sup>1</sup>H-NMR, <sup>13</sup>C-NMR evaluates the carbon and hydrogen environment in the whole portion of the bio-oil, in the molecular level. The environment of the carbon and hydrogen also alter because of changes in different organic groups and compounds attached to them. Furthermore, changes in pyrolysis temperatures also bring significant variation in carbon and hydrogen environment in the overall bio-oil.

#### 3.5.1. <sup>1</sup>H-NMR analysis of SCSW-bio-oils

Fig. 6 and Table 4 presents the <sup>1</sup>H-NMR spectra of bio-oils obtained from pyrolysis of SCSW at various temperatures. The aliphatic region ranging from 0 to 3 ppm shows the crowding of peaks corresponding to aliphatic protons as compared to other regions in the downfield shift. The similar kind of spectral pattern was also noticed in the <sup>1</sup>H-NMR analysis of switchgrass and chicken litter (Mullen et al., 2009). As the temperature increased from 300 to 400 °C, the proportions of aliphatic protons reduced from 63 % to 56 %, but further increase in temperature exhibited maximum aliphatic protons i.e., 66.4 % in the region 0–2.2 ppm as shown in Table 4. It is also noticed that the peak intensities at 1.3, 1.7 and 2.1 ppm increased significantly at higher pyrolysis temperatures. The region 2.2–3 ppm corresponds to CH<sub>3</sub>-Ar α or CH<sub>3</sub>=O protons, which got slightly reduced from 9.3 % to 8 %, with changes in pyrolysis temperature from 300 to 500 °C. The sharp singlet at 2.5 ppm corresponds to dmso-d<sub>6</sub> peak, which is excluded from the analysis.

The protons linked to methylene dibenzene groups or alcohols fall into the range of 3–4.2 ppm. The peak at 3.5 ppm represents the trapped water molecule found in the SCSW-bio-oils obtained at 300 and 500 °C, indicating the enhanced dehydration reactions at higher temperature. Similarly, there are traces of moisture arising from the deuterated solvent are also detected at 3.5 ppm.

The methoxy protons or Ar-CH<sub>2</sub>-O-R protons in the region 4.2–6.4 ppm show mild presence in at 300 and 500 °C while maximum O-CH<sub>3</sub> proportions (8.7 %) was observed at 400 °C. The region 6.4–8.5 ppm correlates to the protons attached to aryl group or saturated carbon as shown by scattered triplets at 6.5, 6.8 and 7.2 ppm and the intensity of these triplets reduced as the temperature increased from 300 to 500 °C. The region 8.5–10 ppm corresponds to protons associated with COOH and CHO and scattered mini peaks are evident ranging from 1 to 3.5 % due to the presence of carbonyl species in the SCSW-bio-oil. <sup>1</sup>H-NMR analysis showed more aliphatic protons and protons pertaining to heteroaromatic compounds are prevalent in the SCSW bio-oils.

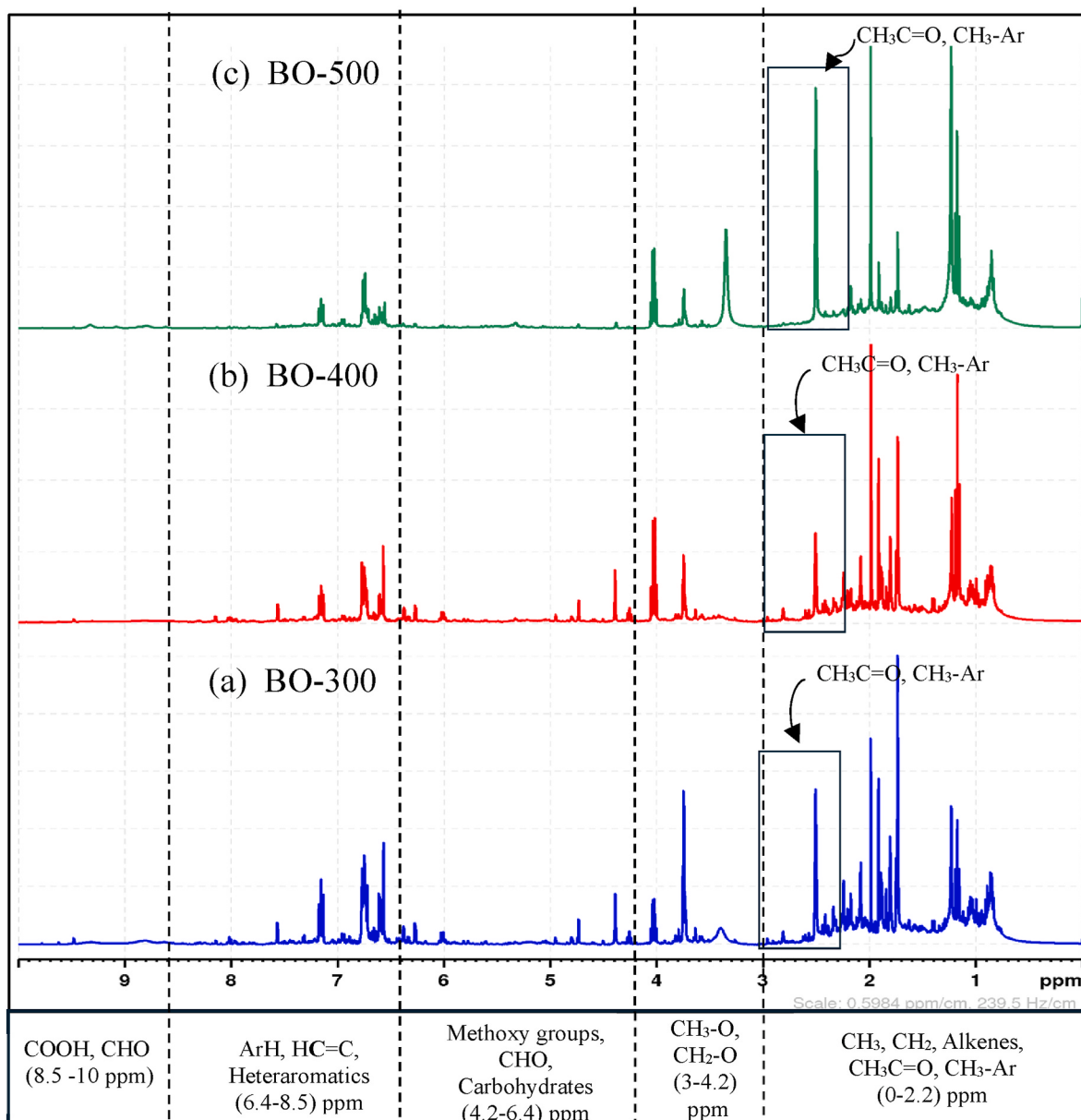


**Fig. 6.**  $^1\text{H}$ -NMR analysis of SCSW bio-oils obtained at various pyrolysis temperatures (a) 300 °C (b) 400 °C (c) 500 °C.

**Table 4**  
 $^1\text{H}$ -NMR analysis of SCSW-bio-oils at various temperatures.

$^1\text{H}$ -NMR Analysis of SCSW-bio-oils		% Area		
Region	Proton Assignment	BO-300	BO-400	BO-500
0–2.2	CH <sub>3</sub> , CH <sub>2</sub> and Alkanes, aliphatic protons	63.75	56.77	66.4
2.2–3.0	CH <sub>3</sub> C=O, CH <sub>3</sub> -Ar, -CH <sub>2</sub> -Ar or heteroatoms	9.3	8.8	8
3.0–4.2	CH <sub>3</sub> O, -CH <sub>2</sub> O, Alcohols, and probable presence of Methylene dibenzene	8.07	15.04	12.5
4.2–6.4	CHO, Ar OH, HC=C, Methoxy groups or carbohydrates	3.88	8.71	3
6.4–8.5	ArH, HC=C (Conjugated), Heteroaromatics	13.5	13	9
8.5–10	COOH, CHO	1.5	3.35	1

### 3.5.2. $^{13}\text{C}$ -NMR analysis of SCSW bio-oils

Fig. 7 and Table 5 present the  $^{13}\text{C}$ -NMR spectrum of SCSW bio-oils obtained at various temperatures. It is noticed that there is massive herding of peaks in two regions: 0–55 ppm and 105–160 ppm, reflecting

the aliphatic and aromatic nature of SCSW bio-oils respectively. In the  $^{13}\text{C}$ -NMR spectrogram, the regions between 55–80 ppm and 170–180 ppm exhibit minimal crowding, characterized by singlets of differing intensities corresponds to methoxy and carbonyl carbons respectively (Hao et al., 2016). In the 0–55 region, the increase in peaks heights indicates the enhancement of aliphatic nature with increasing temperatures. Similar can be confirmed from Table 5 where long and branched chain aliphatics are increased from 9.49 to 18.31 % with an increase in pyrolysis temperatures from 300 to 500 °C. In 55–95 ppm, %carbon associated with ethers, sugars and alcoholic species are increased from 0.68 to 22 % with temperature from 300 to 500 °C. Formation of carbohydrate or methoxy species in the region 55–95 ppm at the higher pyrolysis temperatures is accompanied by the release of the byproducts such as water that aptly confirms the higher water content in the SCSW-bio-oil at 500 °C.

The region 95–165 ppm relates to the carbon associated with aromatic and furanic character of the bio-oil. The peaks at 112.5, 120 and 130 ppm exhibit maximum intensity in SCSW bio-oils obtained at all temperature (300–500 °C), representing the carbon arising from cyclic

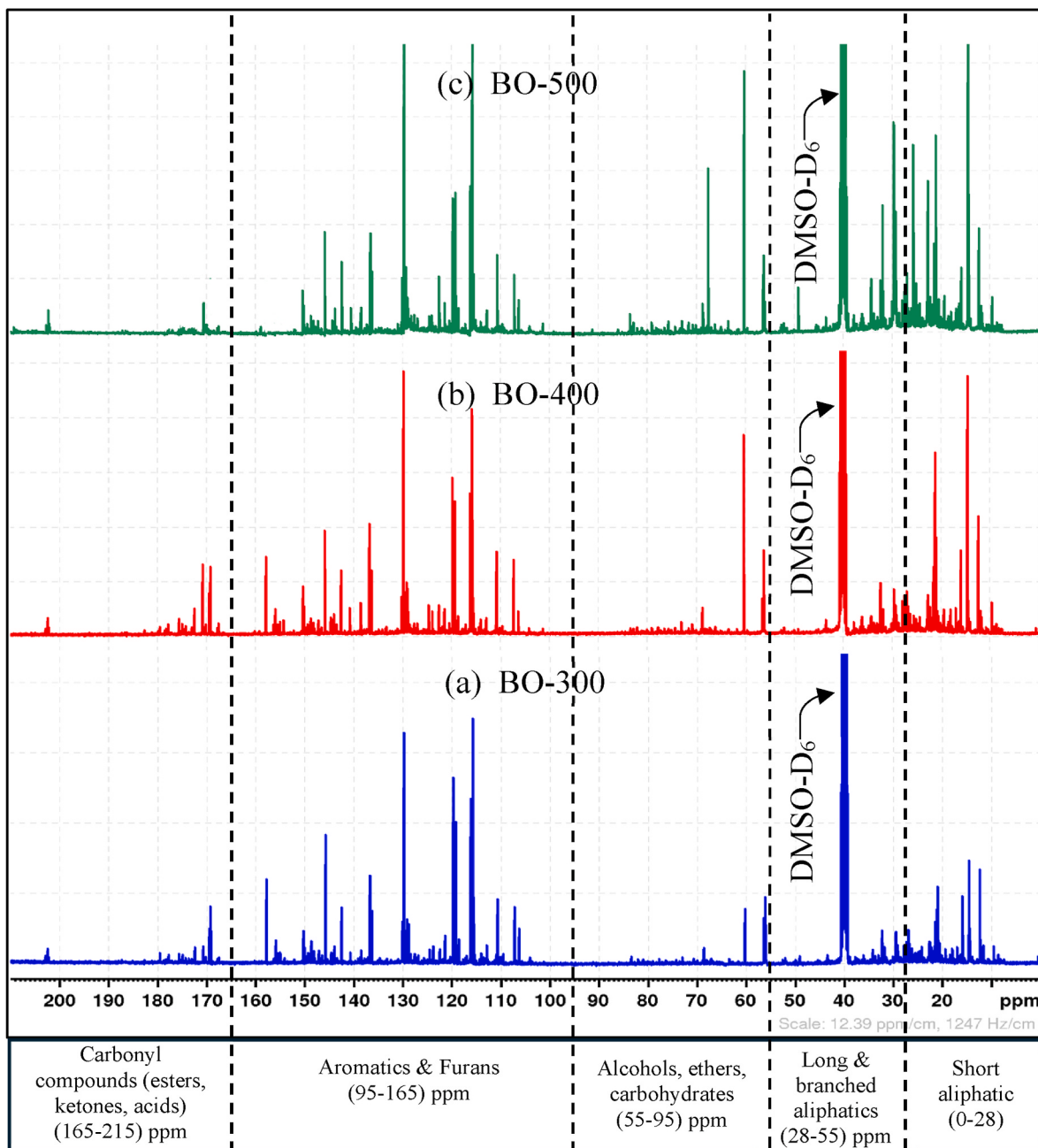


**Fig. 7.**  $^{13}\text{C}$ -NMR analysis of SCSW bio-oils obtained at (a) 300 °C (b) 400 °C (c) 500 °C.

**Table 5**  
 $^{13}\text{C}$ -NMR analysis of SCSW-bio-oils at various temperatures.

$^{13}\text{C}$ -NMR Analysis of SCSW-bio-oils		% Area		
Region	Carbon Assignment	BO-300	BO-400	BO-500
0-28	Short Aliphatics	26.02	20.32	22.68
28-55	Long and branched aliphatics (excluding solvent peak (dmso-d6))	9.49	14.70	18.31
55-95	Alcohols, ethers, phenolic-methoxys, carbohydrates sugars	0.68	18.19	22.09
95-165	Aromatics, olefins	39.56	34.31	30.59
165-215	Carbonyl species	23	12	3.24

ketones and furanic species. There are 3 peaks with lower intensity at 135, 145 and 157 ppm in this region. The nature of these peaks is affected with temperature therefore the % carbon area of aromatic and furanic region changed from 39.56 % to 30.6 % with increase in p temperatures from 300 to 500 °C.

The region 165–200 ppm relates to the carbons of carbonyl species. It is noticed that the increase in temperature from 300 to 500 °C, reduced the carbonyl content significantly from 23 to 3 %.  $^{13}\text{C}$ -NMR highlighted that SCSW bio-oils have the presence of carbons associated with aliphatic, ketonic, aromatic, furanic and sugars. It is observed that from Fig. 7 and Table 4, that the increase in pyrolysis temperatures has significantly increased the carbons associated with aliphatic and sugar or methoxy species.

### 3.5.3. Application of SCSW bio-oils

The SCSW biooils obtained at various temperatures, majorly contains

bioactive cyclic ketone (1,3-Cyclopentanedione), ranging from 42 to 50 % of SCSW bio-oils. These bioactive cyclic ketones can be used for multiple application including drug design and chemical probes ("1, 3-Cyclopentanedione," n.d.; Hori et al., 2004). Secondly bio-oil rich in cyclic ketones can be converted into dicarboxylic acid using biocatalyst such as *Pseudomonas putida* via biological conversion route (Borchert et al., 2023). These dicarboxylic acids are one of the important platform chemicals used in manufacture of polyesters (Nishikubo and Ozaki, 1990). Table 6 presents a comparison between the bio-oils derived from the pyrolysis of SCSW with other spent essential oil industry waste in terms quantity and quality of bio-oils. It is evident that phenolics are major compounds present in bio-oils obtained from the pyrolysis of spent lemon myrtle waste, spent citronella waste and spent *Cymbopogon flexuosus* waste, whereas SCSW bio-oil showed higher proportions of cyclic ketones along with phenols and cyclic hydrocarbons.

From the above discussion, it is evident that the pyrolysis of essential oil industry waste offers a promising alternative for managing large quantities of solid waste while producing value-added products i.e. bio-oil. However, several challenges remain, including: (i) the separation of individual organic compounds present in the bio-oil, and (ii) the high content of oxygenated compounds in the bio-oil. The separation of these organic compounds from one another represents another important area of research in this field. Various methods have been reported for isolating cyclic ketones from the complex bio-oil mixture, including fractional or multi-stage distillation techniques as well as molecular distillation (Borchert et al., 2023; Wang et al., 2009), liquid-liquid extraction using chloroform as a solvent (Drugkar et al., 2022). The selection of appropriate separation strategies depends on factors such as desired purity levels, processing scale, economic considerations, and downstream applications (Drugkar et al., 2022). The SCSW bio-oil contains oxygenated components, which lowers the bio-oil quality as fuel. Further improvement of SCSW bio-oil obtained at 500 °C can be done by changing the other influential pyrolysis parameters such as heating rates and residence time and by introducing heterogeneous catalysts to reduce the oxygenated species in the bio-oil, making it suitable for drop down fuel applications. Hence, the proposed future work focuses on the isolation of individual organic compounds and the reduction of oxygen content in the bio-oil to enhance its quality and make it suitable for direct use.

#### 4. Conclusion

This work investigated the valorization of spent carrot seed waste via pyrolysis to produce bio-oil at different temperatures ranging from 300 to 500 °C. Proximate analysis showed higher volatile content (71 %) accompanied by higher ash content (13.3 %) and less fixed carbon (8.2 %). The SCSW contains the major proportions of Na, Si and Ca along with Fe and Mg. Elemental analysis exhibited higher levels of carbon and oxygen and TGA/DTG analysis revealed that the maximum devolatilization occurred between 250 and 500 °C. The temperature had positive impact on bio-oil yield of SCSW, resulting maximum yield of 16.6 wt% at 500 °C. GC-MS analysis revealed that 1,3-cyclopentadione (32 %–45 %) is the major bio-oil component present at all temperatures, mainly formed by ring opening, cyclization, decarboxylation and decarbonylation of anhydrosugars and hemicellulose under the influence of inherent metallic species in SCSW. Further, increase in temperature from 300 to 500 °C reduced the hydroxy ketones and furanic species however increased cyclic hydrocarbons along with anhydrosugars. NMR analysis exhibited that SCSW bio-oil obtained at 500 °C showed higher aliphatic, aromatic and carbohydrate nature. The pyrolysis temperature of 500 °C can be considered optimum in terms of yield as well as the quality of bio-oil. The SCSW bio-oil contains oxygenated components, which lowers the bio-oil quality as fuel. Further improvement of SCSW bio-oil obtained at 500 °C can be done by changing the other influential pyrolysis parameters such as heating rates and residence time and by introducing heterogeneous catalysts to reduce

**Table 6**

Qualitative and quantitative comparison of SCSW-bio-oil with various spent biomass feedstocks.

Reference	Raw material	Pyrolysis Temperature	% Bio-oil yield	Bio-oil composition
Abu Bakar et al. (2020)	Spent Lemon Myrtle waste	350–550 °C.	Max bio-oil yield @ 350 °C = 40 wt%	Major fractions of phenolic compounds (32–42 %) across all the temperatures
Kaur et al. (2022)	Spent Citronella waste	300–500 °C.	Max bio-oil yield @ 450 °C = 37.7 wt %	Highest phenolic fraction (50–60 %) in the bio-oil obtained @ 450 °C
Deshmukh et al. (2015)	Spent <i>Cymbopogon flexuosus</i>	450–850 °C.	Max bio-oil yield @ 450 °C = 30 wt%	Highest phenolic fraction (20–30 %) in the bio-oil across all the temperatures
This work	Spent Carrot Seed Waste (SCSW)	300–500 °C.	Max bio-oil @ 500 °C = 16.4 wt%	Highest fraction of cyclic ketone (42–50 %) in the bio-oil across all the temperatures

the oxygenated species in the bio-oil, making it suitable for drop down fuel applications.

#### CRediT authorship contribution statement

**Sourodipto Modak:** Writing – original draft, Visualization, Project administration, Methodology, Investigation, Formal analysis, Data curation. **Priyanka Katiyar:** Writing – review & editing, Visualization, Validation, Supervision, Software, Resources, Methodology, Conceptualization. **Dhrubajyoti Talukdar:** Writing – review & editing, Investigation, Formal analysis. **Bappaditya Gole:** Validation, Supervision.

#### Declaration of competing interest

The authors declare that they have no known competing financial interests or personal relationships that could have appeared to influence the work reported in this paper.

#### Acknowledgments

This research did not receive any specific grant from funding agencies in the public, commercial, or not-for-profit sectors.

#### Data availability

Data will be made available on request.

#### References

- 1,3-Cyclopentanedione 1,3-Cyclopentanedione [WWW Document], n.d. URL <https://www.sigmapelab.com/IN/en/product/aldrich/177164> (accessed 12.14.24).
- Abu Bakar, M.S., Ahmed, A., Jeffery, D.M., Hidayat, S., Sukri, R.S., Mahlia, T.M.I., Jamil, F., Khurrum, M.S., Inayat, A., Moogi, S., Park, Y.K., 2020. Pyrolysis of solid waste residues from Lemon Myrtle essential oils extraction for bio-oil production. *Bioresour. Technol.* 318, 1–5. <https://doi.org/10.1016/j.biortech.2020.123913>.
- Adewuyi, A., 2022. Underutilized lignocellulosic waste as sources of feedstock for biofuel production in developing countries. *Front. Energy Res.* 10, 1–21. <https://doi.org/10.3389/fenrg.2022.741570>.
- Basu, P., 2018. Chapter 3 - biomass characteristics. In: P.B.T.-B.G (Ed.), *Basu Pyrolysis and Torrefaction*, third ed. Academic Press, pp. 49–91. <https://doi.org/10.1016/B978-0-12-812992-0.00003-0>.
- Biswas, B., Pandey, N., Bisht, Y., Singh, R., Kumar, J., Bhaskar, T., 2017. Pyrolysis of agricultural biomass residues: comparative study of corn cob, wheat straw, rice

- straw and rice husk. *Bioresour. Technol.* 237, 57–63. <https://doi.org/10.1016/j.biortech.2017.02.046>.
- Borchert, A.J., Wilson, A.N., Michener, W.E., Roback, J., Henson, W.R., Ramirez, K.J., Beckham, G.T., 2023. Biological conversion of cyclic ketones from catalytic fast pyrolysis with *Pseudomonas putida* KT2440. *Green Chem.* 25, 3278–3291. <https://doi.org/10.1039/d3gc00084b>.
- Casti, J., He, Y., Yu, X., Banks, S.W., Yang, Y., Zhang, X., Yu, Y., Liu, R., Bridgwater, A.V., 2017. Review of physicochemical properties and analytical characterization of lignocellulosic biomass. *Renew. Sustain. Energy Rev.* 76, 309–322. <https://doi.org/10.1016/j.rser.2017.03.072>.
- Casoni, A.I., Gutierrez, V.S., Volpe, M.A., 2019. Conversion of sunflower seed hulls, waste from edible oil production, into valuable products. *J. Environ. Chem. Eng.* 7, 102893. <https://doi.org/10.1016/j.jece.2019.102893>.
- Collard, F.X., Blin, J., 2014. A review on pyrolysis of biomass constituents: mechanisms and composition of the products obtained from the conversion of cellulose, hemicelluloses and lignin. *Renew. Sustain. Energy Rev.* 38, 594–608. <https://doi.org/10.1016/j.rser.2014.06.013>.
- Deshmukh, Y., Yadav, V., Nigam, N., Yadav, A., Khare, P., 2015. Quality of bio-oil by pyrolysis of distilled spent of *Cymbopogon flexuosus*. *J. Anal. Appl. Pyrolysis* 115, 43–50. <https://doi.org/10.1016/j.jap.2015.07.003>.
- Drugkar, K., Rathod, W., Sharma, T., Sharma, A., Joshi, J., Pareek, V.K., Ledwani, L., Diwekar, U., 2022. Advanced separation strategies for up-gradation of bio-oil into value-added chemicals: a comprehensive review. *Sep. Purif. Technol.* 283, 120149. <https://doi.org/10.1016/j.seppur.2021.120149>.
- Efika, C.E., Onwudili, J.A., Williams, P.T., 2018. Influence of heating rates on the products of high-temperature pyrolysis of waste wood pellets and biomass model compounds. *Waste Manag.* 76, 497–506. <https://doi.org/10.1016/j.wasman.2018.03.021>.
- Essential Oils Market Key Drivers, Restraints and Winning Strategies | MarketsandMarkets™ [WWW Document], n.d. URL <https://www.marketsandmarkets.com/Market-Reports/essential-oil-market-119674487.html> (accessed 4.3.23).
- Fadeyi, A.E., Akiode, S.O., 2023. Analysis and characterization of lignocellulosic biomass extracted from selected agricultural wastes. In: Jacob-Lopes, E., Zepka, L.Q., Dias, R. R. (Eds.), IntechOpen, Rijeka. <https://doi.org/10.5772/intechopen.112954>. Ch. 2.
- Gao, Y., Ozel, M.Z., Dugmore, T., Sulaeman, A., Matharu, A.S., 2021. A biorefinery strategy for spent industrial ginger waste. *J. Hazard. Mater.* 401, 123400. <https://doi.org/10.1016/j.jhazmat.2020.123400>.
- Gautam, R., Vinu, R., 2020. Reaction engineering and kinetics of algae conversion to biofuels and chemicals: via pyrolysis and hydrothermal liquefaction. *React. Chem. Eng.* 5, 1320–1373. <https://doi.org/10.1039/dore00084a>.
- Hakeem, I.G., Halder, P., Marzbali, M.H., Patel, S., Kundu, S., Paz-Ferreiro, J., Surapaneni, A., Shah, K., 2021. Research progress on levoglucosan production via pyrolysis of lignocellulosic biomass and its effective recovery from bio-oil. *J. Environ. Chem. Eng.* 9, 105614. <https://doi.org/10.1016/j.jece.2021.105614>.
- Hao, N., Ben, H., Yoo, C.G., Adhikari, S., Ragauskas, A.J., 2016. Review of NMR characterization of pyrolysis oils. *Energy Fuels* 30, 6863–6880. <https://doi.org/10.1021/acs.energyfuels.6b01002>.
- Hori, H., Nagasawa, H., Uto, Y., Ohkura, K., Kirk, K.L., Uehara, Y., Shimamura, M., 2004. Design of hypoxia-targeting protein tyrosine kinase inhibitor using an innovative pharmacophore 2-methylene-4-cyclopentene-1,3-dione. *Biochim. Biophys. Acta, Proteins Proteomics* 1697, 29–38. <https://doi.org/10.1016/j.bbapap.2003.11.011>.
- Hsu, C.P., Huang, A.N., Kuo, H.P., 2015. Analysis of the rice husk pyrolysis products from a fluidized bed reactor. *Procedia Eng.* 102, 1183–1186. <https://doi.org/10.1016/j.proeng.2015.01.244>.
- Hu, X., Gholizadeh, M., 2019. Biomass pyrolysis: a review of the process development and challenges from initial researches up to the commercialisation stage. *J. Energy Chem.* 39, 109–143. <https://doi.org/10.1016/j.jechem.2019.01.024>.
- Hu, Y., Wang, H., Lakshmikanand, M., Wang, S., Wang, Q., He, Z., Abomohra, A.E.F., 2021. Catalytic co-pyrolysis of seaweeds and cellulose using mixed ZSM-5 and MCM-41 for enhanced crude bio-oil production. *J. Therm. Anal. Calorim.* 143, 827–842. <https://doi.org/10.1007/s10973-020-09291-w>.
- Huang, Y.F., Kuan, W.H., Chiueh, P.T., Lo, S.L., 2011. Pyrolysis of biomass by thermal analysis-mass spectrometry (TA-MS). *Bioresour. Technol.* 102, 3527–3534. <https://doi.org/10.1016/j.biortech.2010.11.049>.
- Huo, E., Duan, D., Lei, H., Liu, C., Zhang, Y., Wu, J., Zhao, Y., Huang, Z., Qian, M., Zhang, Q., Lin, X., Wang, C., Mateo, W., Villota, E.M., Ruan, R., 2020. Phenols production form Douglas fir catalytic pyrolysis with MgO and biomass-derived activated carbon catalysts. *Energy* 199, 1–29. <https://doi.org/10.1016/j.energy.2020.117459>.
- India: petroleum products import value 2023 | Statista [WWW Document], n.d. URL <https://www.statista.com/statistics/625218/import-value-of-petroleum-india/> (accessed 12.10.24).
- Kakkur, S., Naidu, S., Bhatt, M., Chakinala, A.G., Joshi, J., Gautam, S., Mohanty, K., Kataria, G., Sharma, A., 2023. Pyrolytic conversion of agricultural residue using continuous auger reactor for resource recovery. *J. Anal. Appl. Pyrolysis* 171, 105951. <https://doi.org/10.1016/j.jap.2023.105951>.
- Karnjanakom, S., Chaihad, N., Kongparakul, S., Samart, C., Abudula, A., Guan, G., 2020. In: Fang, Z., Smith Jr, R.L., Xu, L. (Eds.), *Catalytic Upgrading of Bio-Oils into Aromatic Hydrocarbon over Highly Active Solid Catalysts BT - Production of Biofuels and Chemicals with Pyrolysis*. Springer Singapore, Singapore, pp. 141–162. [https://doi.org/10.1007/978-981-15-2732-6\\_5](https://doi.org/10.1007/978-981-15-2732-6_5).
- Kaur, R., Kumar, A., Biswas, B., Krishna, B.B., Bhaskar, T., 2022. Investigations into pyrolytic behaviour of spent citronella waste: slow and flash pyrolysis study. *Bioresour. Technol.* 366, 12820. <https://doi.org/10.1016/j.biortech.2022.128202>.
- Kelkar, S., Saffron, C.M., Chai, L., Boeve, J., Stuecken, T.R., Garedew, M., Li, Z., Kriegel, R.M., 2015. Pyrolysis of spent coffee grounds using a screw-conveyor reactor. *Fuel Process. Technol.* 137, 170–178. <https://doi.org/10.1016/j.fuproc.2015.04.006>.
- Li, S., Xu, S., Liu, S., Yang, C., Lu, Q., 2004. Fast pyrolysis of biomass in free-fall reactor for hydrogen-rich gas. *Fuel Process. Technol.* 85, 1201–1211. <https://doi.org/10.1016/j.fuproc.2003.11.043>.
- Li, C., Sun, Y., Zhang, S., Wang, Y., Xiang, J., Hu, S., Wang, S., Hu, X., 2021. Pyrolysis of sesame residue: evolution of the volatiles and structures of biochar versus temperature. *Environ. Technol. Innov.* 24, 101859. <https://doi.org/10.1016/j.eti.2021.101859>.
- Li, P., Wan, K., Chen, H., Zheng, F., Zhang, Z., Niu, B., Zhang, Y., Long, D., 2022. Value-added products from catalytic pyrolysis of lignocellulosic biomass and waste plastics over biochar-based catalyst: a state-of-the-art review. *Catalysts* 12. <https://doi.org/10.3390/catal12091067>.
- Maulinda, L., Husin, H., Rahman, N.A., Rosnelly, C.M., Nasution, F., Abidin, N.Z., Faisal, Yani, F.T., Ahmadi, 2023. Effects of temperature and times on the product distribution of bio-oils derived from *Typha latifolia* pyrolysis as renewable energy. *Results Eng.* 18, 101163. <https://doi.org/10.1016/j.rineng.2023.101163>.
- Mishra, R.K., Mohanty, K., 2018. Characterization of non-edible lignocellulosic biomass in terms of their candidacy towards alternative renewable fuels. *Biomass Convers. Biorefinery* 8, 799–812. <https://doi.org/10.1007/s13399-018-0332-8>.
- Modak, S., Katiyar, P., Yadav, S., Hans, A., 2023. Valorization of lignocellulosic solid waste obtained from essential oil industry for bio-oil production and dye removal. *Water Pract. Technol.* 18, 2384–2400. <https://doi.org/10.2166/wpt.2023.154>.
- Mullen, C.A., Strahan, G.D., Boateng, A.A., 2009. Characterization of various fast-pyrolysis bio-oils by NMR spectroscopy. *Energy Fuels* 23, 2707–2718. <https://doi.org/10.1021/ef801048b>.
- Nishikubo, T., Ozaki, K., 1990. Synthesis of polyesters by the reaction of dicarboxylic acids with alkyl dihalides using the DBU method. *Polym. J.* 22, 1043–1050. <https://doi.org/10.1295/polymj.22.1043>.
- Perera, F., 2018. Pollution from fossil-fuel combustion is the leading environmental threat to global pediatric health and equity: solutions exist. *Int. J. Environ. Res. Publ. Health* 15. <https://doi.org/10.3390/ijerph1510016>.
- Preethi, Ganasekaran, M., Kumar, G., Karthikeyan, O.P., Varjani, S., Rajesh Banu, J., 2021. Lignocellulosic biomass as an optimistic feedstock for the production of biofuels as valuable energy source: techno-Economic analysis, environmental impact analysis, breakthrough and perspectives. *Environ. Technol. Innov.* 24, 102080. <https://doi.org/10.1016/j.eti.2021.102080>.
- Priyanka, Subbaramaiah, V., Srivastava, V.C., Mall, I.D., 2014. Catalytic oxidation of nitrobenzene by copper loaded activated carbon. *Sep. Purif. Technol.* 125, 284–290. <https://doi.org/10.1016/j.seppur.2014.01.045>.
- Rajpoot, L., Tagade, A., Deshpande, G., Verma, K., Geed, S.R., Patle, D.S., Sawarkar, A.N., 2022. An overview of pyrolysis of de-oiled cakes for the production of biochar, bio-oil, and pyro-gas: current status, challenges, and future perspective. *Bioresour. Technol. Rep.* 19, 101205. <https://doi.org/10.1016/j.biteb.2022.101205>.
- Rangel, M. do C., Mayer, F.M., Carvalho, M. da S., Saboia, G., de Andrade, A.M., 2023. Selecting catalysts for pyrolysis of lignocellulosic biomass. *Biomass* 3, 31–63. <https://doi.org/10.3390/biomass3010003>.
- Roostazadeh, R., Behzad, T., Karimi, K., 2022. Isolation and characterization of lignin-rich particles as byproducts of bioethanol production from wheat straw to reinforce starch composite films. *Ind. Crops Prod.* 186, 115175. <https://doi.org/10.1016/j.indcrop.2022.115175>.
- Saikia, N., Bardalai, M., 2018. Thermal analysis and kinetic parameters determination of biomass using differential thermal gravimetric analysis in N2 atmosphere. *Mater. Today Proc.* 5, 2146–2156. <https://doi.org/10.1016/j.matpr.2017.09.212>.
- Saravanan, A., Yaashikaa, P.R., Kumar, P.S., Thamarai, P., Deivayananai, V.C., Rangasamy, G., 2023. A comprehensive review on techno-economic analysis of biomass valorization and conventional technologies of lignocellulosic residues. *Ind. Crops Prod.* 200, 116822. <https://doi.org/10.1016/j.indcrop.2023.116822>.
- Sieniawska, E., Świątek, Ł., Rajtar, B., Koziol, E., Polz-Dacewicz, M., Skalicka-Woźniak, K., 2016. Carrot seed essential oil—Source of carotol and cytotoxicity study. *Ind. Crops Prod.* 92, 109–115. <https://doi.org/10.1016/j.indcrop.2016.08.001>.
- Silva, C.M., Ferreira, A.F., Dias, A.P., Costa, M., 2016. A comparison between microalgae virtual biorefinery arrangements for bio-oil production based on lab-scale results. *J. Clean. Prod.* 130, 58–67. <https://doi.org/10.1016/j.jclepro.2015.09.053>.
- Varma, A.K., Mondal, P., 2016. Physicochemical characterization and pyrolysis kinetic study of sugarcane bagasse using thermogravimetric analysis. *J. Energy Resour. Technol. Trans. ASME* 138, 1–11. <https://doi.org/10.1115/1.4032729>.
- Varol, E.A., Mutlu, U., 2023. TGA-FTIR analysis of biomass samples based on the thermal Energies 16, 1–19.
- Vasu, H., Wong, C.F., Vijayaretnam, N.R., Chong, Y.Y., Thangalazhy-Gopakumar, S., Gan, S., Lee, L.Y., Ng, H.K., 2020a. Insight into Co-pyrolysis of Palm Kernel Shell (PKS) with Palm Oil Sludge (POS): effect on bio-oil yield and properties. *Waste Biomass Valoriz.* 11, 5877–5889. <https://doi.org/10.1007/s12649-019-00852-1>.
- Vasu, H., Wong, C.F., Vijayaretnam, N.R., Chong, Y.Y., Thangalazhy-Gopakumar, S., Gan, S., Lee, L.Y., Ng, H.K., 2020b. Insight into Co-pyrolysis of Palm Kernel Shell (PKS) with Palm Oil Sludge (POS): effect on bio-oil yield and properties. *Waste Biomass Valoriz.* 11, 5877–5889. <https://doi.org/10.1007/s12649-019-00852-1>.
- Veiga, T.R.L.A., Lima, J.T., Dessimoni, A.L. da A., Pego, M.F.F., Soares, J.R., Trugilho, P. F., 2017. Caracterização de diferentes biomassas vegetais para produção de biocarvões. *Cerne* 23, 529–536. <https://doi.org/10.1590/01047760201723042373>.
- Vuppalaadiyam, A.K., Varsha Vuppalaadiyam, S.S., Sikarwar, V.S., Ahmad, E., Pant, K. K., S, M., Pandey, A., Bhattacharya, S., Sarmah, A., Leu, S.Y., 2023. A critical review on biomass pyrolysis: reaction mechanisms, process modeling and potential challenges. *J. Energy Inst.* 108. <https://doi.org/10.1016/j.joei.2023.101236>.

- Wan, Z., Wang, S., Li, Z., Yi, W., Zhang, A., Li, Y., Zhang, P., 2022. Co-pyrolysis of lignin and spent bleaching clay: insight into the catalytic characteristic and hydrogen supply of spent bleaching clay. *J. Anal. Appl. Pyrolysis* 163, 105491. <https://doi.org/10.1016/j.jaap.2022.105491>.
- Wang, S., Gu, Y., Liu, Q., Yao, Y., Guo, Z., Luo, Z., Cen, K., 2009. Separation of bio-oil by molecular distillation. *Fuel Process. Technol.* 90, 738–745. <https://doi.org/10.1016/j.fuproc.2009.02.005>.
- Wang, S., Mandfloen, P., Jónsson, P., Yang, W., 2021. Synergistic effects in the copyrolysis of municipal sewage sludge digestate and salix: reaction mechanism, product characterization and char stability. *Appl. Energy* 289, 116687. <https://doi.org/10.1016/j.apenergy.2021.116687>.
- Wang, W., Lemaire, R., Bensakhria, A., Luart, D., 2022. Review on the catalytic effects of alkali and alkaline earth metals (AAEMs) including sodium, potassium, calcium and magnesium on the pyrolysis of lignocellulosic biomass and on the co-pyrolysis of coal with biomass. *J. Anal. Appl. Pyrolysis* 163, 105479. <https://doi.org/10.1016/j.jaap.2022.105479>.
- Yaashikaa, P.R., Senthil Kumar, P., Varjani, S., 2022. Valorization of agro-industrial wastes for biorefinery process and circular bioeconomy: a critical review. *Bioresour. Technol.* 343, 126126. <https://doi.org/10.1016/j.biortech.2021.126126>.
- Yi, Q., Qi, F., Cheng, G., Zhang, Y., Xiao, B., Hu, Z., Liu, S., Cai, H., Xu, S., 2013. Thermogravimetric analysis of co-combustion of biomass and biochar. *J. Therm. Anal. Calorim.* 112, 1475–1479. <https://doi.org/10.1007/s10973-012-2744-1>.
- Zadeh, Z.E., Abdulkhani, A., Aboelazayem, O., Saha, B., 2020. Recent insights into lignocellulosic biomass pyrolysis: a critical review on pretreatment, characterization, and products upgrading. *Processes* 8. <https://doi.org/10.3390/pr8070799>.